CHEMISTRY
A EUROPEAN JOURNAL

Metallophilicity versus π–π Interactions: Ligand-Unsupported Argentophilicity/Cuprophilicity in Oligomers-of-Dimers $[M_2L_2]_n$ ($M = Cu^I$ or Ag^I, L = tridentate ligand)

Jie-Peng Zhang,[a] Yi-Bo Wang,[b] Xiao-Chun Huang,[a] Yan-Yong Lin,[a] and Xiao-Ming Chen*[a]

Abstract: To verify whether attractive metallophilic interactions exist in the dimer-of-dimers $[Cu_2(ophen)_2]_2$ (Hophen = 1*H*-[1,10]phenanthrolin-2-one) (**1**), we designed and synthesized a series of such $[M_2L_2]_2$ structures by varying the d^{10} metal and/or the ligand ($M = Cu^I$ or Ag^I, L = ophen or obpy; Hobpy = 1*H*-[2,2′]bipyridinyl-6-one), and have successfully obtained three dimers-of-dimers: $[Ag_2(ophen)_2]_2 \cdot 6\,H_2O$ (**2**), $[Cu_2(obpy)_2]_2$ (**3**), and $[Ag_2(obpy)_2]_2 \cdot 4.5\,H_2O \cdot 0.5\,DMF$ (**4**). X-ray analyses of these structures show that interdimer M–M separations in $[Ag_2(ophen)_2]_2$ (3.199 Å) are remarkably shorter than those in $[Cu_2(ophen)_2]_2$ (3.595 Å). Shorter interdimer M–M separations are found in the structures of $[M_2(obpy)_2]_2$ (2.986 and 2.993 Å in $[Cu_2(obpy)_2]_2$, 3.037 to 3.093 Å in $[Ag_2(obpy)_2]_2$), in which the π systems are smaller than in the complexes with the ophen ligand. Detailed structural comparison of these dimers-of-dimers indicates that the interdimer, face-to-face π–π interactions repulse rather than support the interdimer metal–metal attractive interactions. This study also yields qualitative comparison of the strengths between argentophilic, cuprophilic, and face-to-face π–π interactions. DFT calculations on the four dimers-of-dimers further support the above deduction. The structure of a trimer-of-dimers $[Ag_2(obpy)_2]_3$ (Ag–Ag 3.171 to 3.274 Å) is further evidence that the oligomerization of the $[M_2L_2]$ molecules is favored by stronger metallophilic and weaker face-to-face π–π interactions.

Keywords: argentophilicity · cuprophilicity · density functional calculations · pi interactions · solid-state structures

Introduction

Extensive attention has been focused on the attractive interactions between formally closed-shell (such as d^{10} or s^2) metal centers.[1–17] The term "aurophilicity" has been coined to describe the gold(I)–gold(I) bonding interaction, which is theoretically attributed to correlation and relativistic effects.[2–8] Most structurally characterized short metal–metal contacts of Ag^I/Cu^I complexes are associated with ligand-bridged,[9] network-restricted,[10] or coulombic effects,[11] and only a few reliable cases of argentophilicity and cuprophilicity have been reported; in fact, examples for Cu^I are exceedingly rare.[12–15] Although Ag^I and Cu^I afford rich coordination geometries; most ligand-unsupported examples consist of linear two-coordinate metal centers.[12–14] Theoretical studies on dimeric models of linear two-coordinate complexes indicate that metallophilicity decreases as $Au^I > Ag^I > Cu^I$;[16] however, this area may require further investigation under different levels of theory and other models (coordination geometries).[17] For example, it was claimed very recently that the strengths of metallophilic bonding of the coinage metals may have to be reversed.[17b] The strength of aurophilicity (7–11 $kcal\,mol^{-1}$), being comparable to that of a typical hydrogen bond, can be measured by experiment,[6–8] and is strong enough to influence the overall supramolecular structure; on the other hand argentophilicity/cuprophilicity is relatively weak, and is easily confused by other intermolecular interactions such as hydrogen bonds or π–π interactions.

---

[a] J.-P. Zhang, X.-C. Huang, Y.-Y. Lin, Prof. Dr. X.-M. Chen
School of Chemistry and Chemical Engineering
Sun Yat-Sen University, Guangzhou 510275 (China)
Fax: (+86) 20-8411-2245
E-mail: cescxm@zsu.edu.cn

[b] Prof. Dr. Y.-B. Wang
Department of Chemistry, Guizhou University
Key Laboratory of Guizhou
High-Performance Computational Chemistry
Guiyang 550025 (China)

Supporting information for this article is available on the WWW under http://www.chemeurj.org/ or from the author.

DOI: 10.1002/chem.200400756

Aside from the short metal–metal distance, the construction of d^{10} metal complexes with ligand-unsupported argentophilicity/cuprophilicity to give concrete evidence directly from crystal structural investigation remains a great challenge.

Our recent studies on the hydrothermal hydroxylation of 2,2′-bipyridine-like ligands have established a convenient method for the synthesis of 1*H*-[1,10]phenanthrolin-2-one (designated as Hophen) from 1,10-phenanthroline (phen), as well as 1*H*-[2,2′]bipyridinyl-6-one (Hobpy) from 2,2′-bipyridine (bpy).[18] The two new ligands can easily form dimeric $[M_2L_2]$ structures ($M = Ag^I$ or Cu^I; L = ophen or obpy) with Ag^I or Cu^I ions.[18b,c] The coordination environment in the $[M_2L_2]$ complexes is better described as two T-shaped coordinated metal centers sharing a short intradimer metal–metal contact to accomplish square-planar coordination spheres. Such intramolecular metal–metal contacts, comparable to the corresponding metallic atom–atom distances, observed in the $[Ag_2(ophen)_2]$[16c] and three polymorphs of $[Cu_2(ophen)_2]$[18b] are complicated by the bridging ophen ligands, which are not relevant to reliable metallophilicity. On the other hand, this planar structural model can be extended to new supramolecular structures held together by weak interactions to the central metals. For example, anhydrous, highly electroconductive $[Ag_2(ophen)_2]$ featuring a linear stacking array results from Ag–π interactions.[18c] These dimers appear to exclude significantly notable interdimer, ligand-unsupported metallophilicity, since no close intermolecular metal–metal contact exists in the structures of $[Ag_2(ophen)_2]$, and α,β,γ-$[Cu_2(ophen)_2]$. However, only the alignments of $[Ag_2(ophen)_2]$ and α-$[Cu_2(ophen)_2]$ are reasonable for dipole–dipole interactions, while relatively short intermolecular Cu⋯Cu contacts coexisting with face-to-face π–π overlaps between the aromatic moieties were found in β-$[Cu_2(ophen)_2]$ (3.375 Å) and γ-$[Cu_2(ophen)_2]$ (3.595 Å) (Figure S1 in the Supporting Information). Since the intermolecular π–π overlap in γ-$[Cu_2(ophen)_2]$ is more significant than that in β-$[Cu_2(ophen)_2]$, we speculated that the repulsion between the large, aromatic ophen ligands prevent closer intermolecular Cu–Cu contacts. Meanwhile, whether the interdimer Cu–Cu contacts are supported by metallophilic or π–π interactions can hardly be judged by individual structures. Therefore, we require a comparison of a number of structural analogues tuning the abilities of metallophilic and/or π–π interactions. Fortunately, this work has been successfully done within a series of dimers-of-dimers, that is, analogues of γ-$[Cu_2(ophen)_2]$ ($[Cu_2(ophen)_2]_2$ **1**), with variations of d^{10} metals and/or the aromatic ligands, namely $[Ag_2(ophen)_2]_2 \cdot 6H_2O$ (**2**), $[Cu_2(obpy)_2]_2$ (**3**), and $[Ag_2(obpy)_2]_2 \cdot 4.5H_2O \cdot 0.5DMF$ (**4**). The crystal structures of these compounds, along with those of the free ligand Hobpy and an unexpected trimer-of-dimers $[Ag_2(obpy)_2]_3 \cdot 18H_2O$ (**5**), will be presented and discussed in the context of intermolecular metallophilicity.

Abstract in Chinese:

本文为验证亲金属作用是否存在于双二聚体 $[Cu_2(ophen)_2]_2$ (Hophen = 1*H*-邻菲咯啉-2-酮) (**1**)之中，利用不同d^{10}金属和类似配体合成了系列具 $[M_2L_2]_2$ ($M = Cu^I$ 或 Ag^I, L = ophen 或 obpy; Hobpy = 1*H*-2,2'-联吡啶-6-酮)结构的配合物 $[Ag_2(ophen)_2]_2 \cdot 6H_2O$ (**2**), $[Cu_2(obpy)_2]_2$ (**3**) 和 $[Ag_2(obpy)_2]_2 \cdot 4.5H_2O \cdot 0.5DMF$ (**4**)。晶体结构分析表明，$[Ag_2(ophen)_2]_2$ (3.199 Å) 的分子间金属－金属距离比 $[Cu_2(ophen)_2]_2$ (3.595 Å) 中的要短。尽管obpy的π体系比ophen的小，但是 $[M_2(obpy)_2]_2$ ($[Cu_2(obpy)_2]_2$ 2.986, 2.993 Å; $[Ag_2(obpy)_2]_2$ 3.037-3.093 Å) 中分子间金属－金属距离比$[M_2(ophen)_2]_2$中的更短。密度泛函计算结果进一步表明，在这些结构中，二聚体间的面对面π–π作用并非支持而是阻碍分子间金属－金属相互吸引作用。本文报道的三重二聚体$[Ag_2(obpy)_2]_3$进一步说明强的亲金属作用和弱的π–π作用更有利于这些 $[M_2L_2]$ 分子间的聚合。

Results

Synthesis and crystallization strategy: Since attractive argentophilic and cuprophilic interactions are considered to be very weak, the intermolecular metallophilicity will certainly not overwhelm the aggregation of $[M_2L_2]$ molecules. The competition among metallophilicity and other supramolecular interactions such as π–π, Ag–π, and dipole–dipole interactions would lead to a delicate balance in various possible metastable aggregate forms such as $[Ag_2(ophen)_2]$ and polymorphs of $[Cu_2(ophen)_2]$ (Scheme 1). To generate a series of structurally related analogues featuring a similar motif, we tried different reaction conditions in the synthesis and crystallization of such $[M_2L_2]$ compounds. In particular, different crystallization conditions were applied for the silver(I) com-

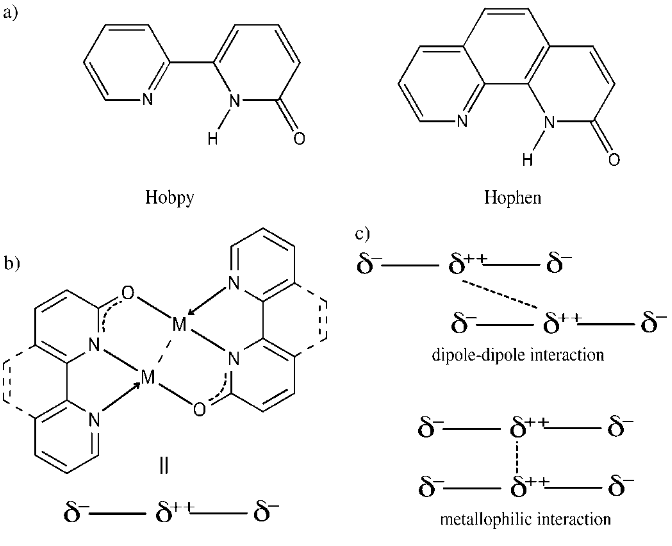

Scheme 1. Structures of a) Hobpy and Hophen, and b) $[M_2L_2]$. c) Possible stacking modes for $[M_2L_2]$.

plexes to avoid the one-dimensional array motif reported previously.[18c] Fortunately, four oligomers-of-dimers (**2**–**5**) structurally similar to $[Cu_2(ophen)_2]_2$ were obtained. It should be noted that only one dimer-of-dimers was isolated for $[Cu_2(obpy)_2]$ (i.e., **3**) in different hydrothermal conditions, while $[Cu_2(ophen)_2]$ is polymorphic.

Crystal structures: The crystal structure of Hobpy·1/6benzene reveals that, like free Hophen, the free Hobpy ligand possesses a ketone (C–O 1.247(2) Å) rather than an hydroxyl form.[18d] The pyridyl moiety of Hobpy rotates 180° to form an *anti*-conformation so as to furnish a dimer through two N–H···O (N···O 2.853(2) Å, N–H···O 167.0°) and two C–H···O (C···O 3.156(3) Å, C–H···O 164.0°) hydrogen bonds (Figure 1). The Hobpy dimers further stack through offset π–π interactions (face-to-face distance ca. 3.45 Å) to form a honeycomb-like structure, and the highly disordered benzene molecules are located in the channels (Figure S2 in the Supporting Information).

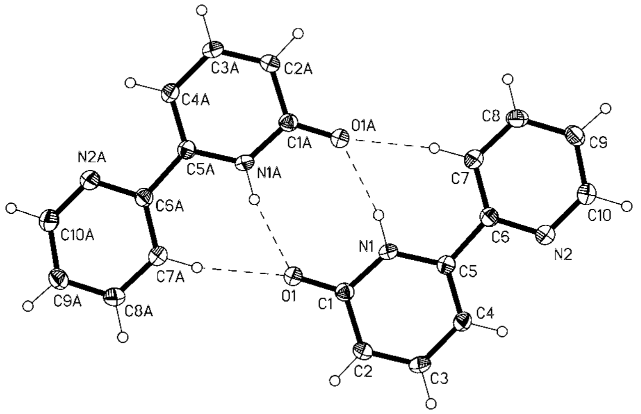

Figure 1. Perspective view of a hydrogen-bonded Hobpy dimer.

Crystal structural analyses reveal that complexes **2**–**5** all consist of the desired $[M_2L_2]$ (M = Ag^I or Cu^I, L = ophen or obpy) structural units. The dimeric $[M_2L_2]$ structures in **2**–**5** are comparable to those found in the related complexes previously reported,[18b,c] while the intramolecular M–M separations in **3** (Cu–Cu 2.5790(5) Å) and **5** (Ag–Ag 2.7452(4)–2.7485(4) Å) are shorter than those found in the other complexes. Like **1**, the $[M_2L_2]$ dimers are further dimerized in **2**–**4**, whereas the $[Ag_2(obpy)_2]$ molecules are associated into a trimer in **5**. Although the lattice solvent molecules are different in **1**–**5**, the complexes display very similar one- and two-dimensional packing patterns (Figure S3 in the Supporting Information), exhibiting similar intermolecular π–π and CH···π interactions. Therefore we can derive information for evaluation of interdimer cuprophilicity and argentophilicity, as well as π–π interactions by structural comparison of these complexes.

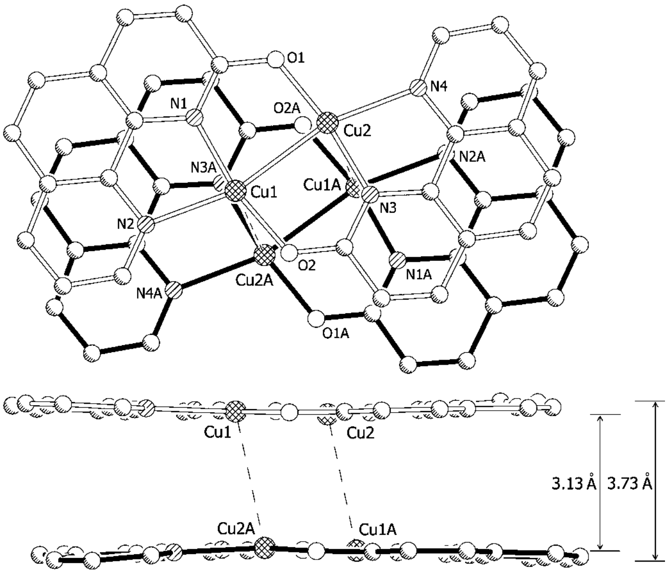

Figure 2. Top (top) and side (bottom) views of $[Cu_2(ophen)_2]_2$ in **1**.

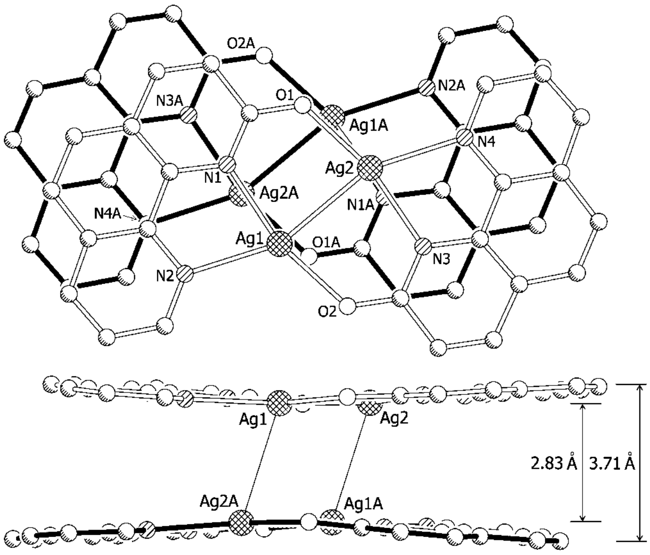

Figure 3. Top (top) and side (bottom) views of $[Ag_2(ophen)_2]_2$ in **2**.

Very similar to the $[Cu_2(ophen)_2]_2$ dimer in **1** (Figure 2), each pair of $[Ag_2(ophen)_2]$ molecules in **2** are related by an inversion center, featuring a slipped face-to-face alignment (type I, Figure 3). The change from Cu^I to Ag^I decreases the two shorter interdimer M–M distances from 3.595 to 3.199 Å. This structural observation demonstrates clearly that argentophilicity is stronger than cuprophilicity. The attractive nature of interdimer Ag–Ag interactions can also be judged by the fact that the edges of the ligands are bent outward, with the pairs of metal atoms facing toward each other. In fact, the mean deviation of all non-hydrogen atoms from a least-squares plane fit to one $[Ag_2(ophen)_2]$ unit in **2** is 0.094 Å and the displacements of the metal atoms from this plane are 0.228 (Ag1) and 0.238 Å (Ag2), whereas these values in **1** are only 0.056 ($[Cu_2(ophen)_2]$), 0.069 (Cu1), and 0.133 Å (Cu2), respectively.

In **3**, centrosymmetric $[Cu_2(obpy)_2]_2$ possesses a new slipped face-to-face conformation (type II, Figure 4), which is

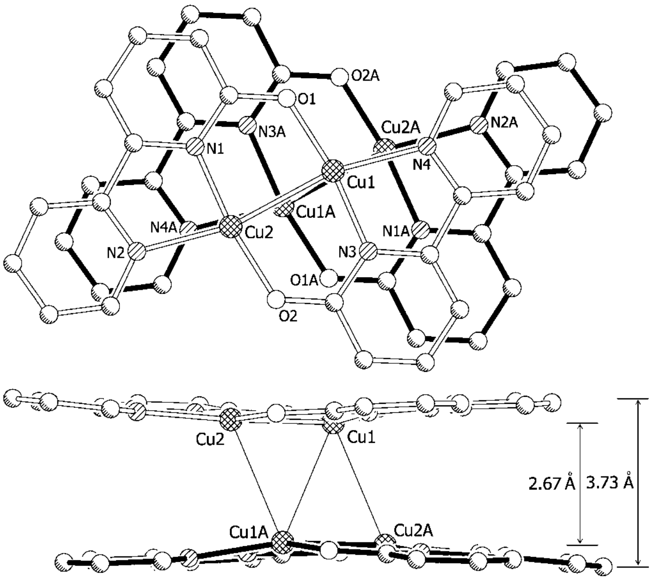

Figure 4. Top (top) and side (bottom) views of $[Cu_2(obpy)_2]_2$ in **3**.

different to the type I arrangement in the direction of slippage. In this dimer-of-dimers, two $[Cu_2(obpy)_2]$ molecules couple by means of three close Cu–Cu contacts (Cu1−Cu2A, Cu2−Cu1A 2.9862(7); Cu1−Cu1A 2.9934(5) Å). The distortions of the originally planar dimeric molecules (deviations: $[Cu_2(obpy)_2]$ 0.096, Cu1 0.459, Cu2 0.307 Å) are more significant than those in **1**, thus providing more remarkable evidence of occurrence of intermolecular cuprophilic interactions. There are only a few ligand-unsupported cuprophilic interactions reported to date; these are usually constructed by linear two-coordinate Cu^I centers, such as $[Cu(NH_3)Cl]$ (2.979(1) Å), $[Cu(NH_3)_2]Br$ (2.931(1) Å),[14a] $([CuCl_2]^-)_2$ (2.922(2) Å),[14b] and $[t\mathrm{Bu}Cu(CN)Li\cdot(OEt_2)_2]_8$ (2.713(1) Å).[14c] To our knowledge, only one example featuring T-shaped coordinated Cu^I centers has been reported in $[Cu_3\{2\text{-}[3(5)\text{-pz}]py\}_3]_2$ (2.905(3) Å), which has a different molecular topology to **3**.[14d]

The dimer-of-dimers conformation of **4** is different to that found in types I and II. The two $[Ag_2(obpy)_2]$ molecules are oriented almost perpendicular to each other in parallel planes (dihedral angle 2.4°, angle between two Ag−Ag vectors 79.1°; type III, Figure 5). There are three close intermolecular Ag–Ag contacts (Ag1−Ag3 3.0228(5), Ag1−Ag4 3.0809(5), Ag2−Ag3 3.0921(5) Å) shorter than the sum of van der Waals radii, which indicate stronger intermolecular argentophilicity than the ophen analogue in **2** (three shorter versus two longer by more than 0.2 Å). The slightly longer interdimer M−M contacts relative to those of the Cu^I analogue **3** do not conflict with the idea that argentophilicity is stronger than cuprophilicity, since Cu^I is much smaller than Ag^I (sum of the van der Waals radii for Cu 2.80 Å, Ag 3.44 Å).[19] The $[Ag_2(obpy)_2]$ molecules in **4** are more bent than the $[Ag_2(ophen)_2]$ molecules in **2** (deviations: $[Ag_2(obpy)_2]$ 0.139 and 0.144, Ag1 0.459, Ag2 0.307, Ag3 0.360, Ag4 0.329 Å).

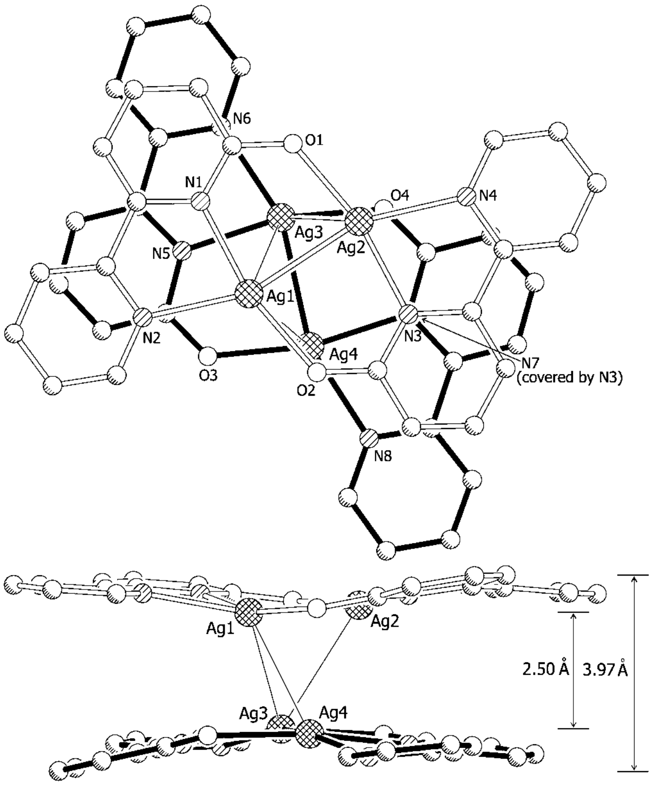

Figure 5. Top (top) and side (bottom) views of $[Ag_2(obpy)_2]_2$ in **4**.

In **5**, two $[Ag_2(obpy)_2]$ molecules, which are almost parallel to each other (dihedral angle 0.6°, angle between the Ag−Ag vectors: 2.8°), join another $[Ag_2(obpy)_2]$ molecule from opposite directions with type III alignment (dihedral angle: 0.6 and 1.0°, angles between the Ag−Ag vectors: 72.4 and 72.6°) similar to that in **4**, to accomplish an unexpected trimer-of-dimers $[Ag_2(obpy)_2]_3$. The middle $[Ag_2(obpy)_2]$ molecule remains basically planar (deviations: $[Ag_2(obpy)_2]$ 0.028, Ag3 0.022, Ag4 −0.024 Å), while the two outer molecules are bent with the edges of obpy distorted outward (Figure 6). Detailed geometric inspection shows that the two outer molecules are rather unsymmetrical and nonplanar, as evident by the intermolecular Ag−Ag separations (Ag2−Ag4 3.1725(4), Ag3−Ag5 3.1713(4), Ag4−Ag5 3.2739(4) Å), as well as their distortions (deviations for the Ag1−Ag2 molecule: $[Ag_2(obpy)_2]$ 0.090, Ag1 0.244, Ag2 0.286 Å; for the Ag5−Ag6 molecule: $[Ag_2(obpy)_2]$ 0.132, Ag5 0.433, Ag6 0.229 Å).

Discussion

Although the short intradimer metal–metal contacts in these oligomers-of-dimers are complicated by ligand bridging effects, the interdimer geometries for the dimers-of-dimers gradually change from **1**–**4** (molecular distortions increase and intermolecular metal–metal distances decrease), indicating more and more significant interdimer metal–metal contacts (Table 1). Crystal packing effects may lead to the con-

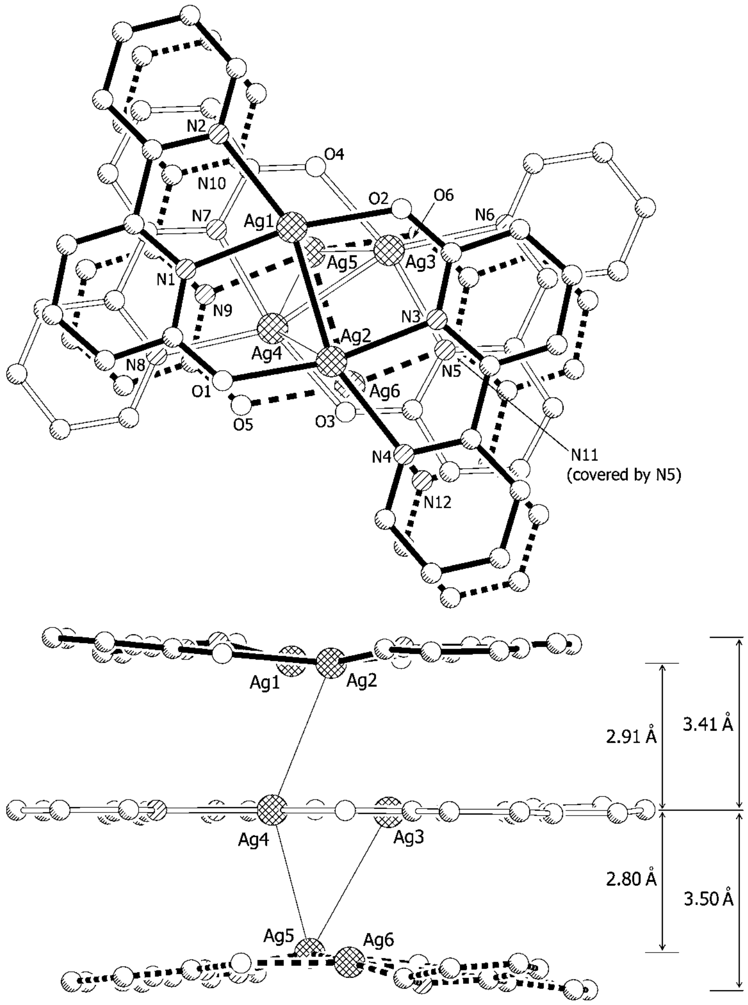

Figure 6. Top (top) and side (bottom) views of $[Ag_2(obpy)_2]_3$ in **5**.

clusion of ligand-unsupported metallophilicity found in individual crystal structures. However, the structural change trends can hardly be rationalized by such weak forces, since the packing patterns for **1**–**5** are rather similar.

The shortest interdimer metal–ligand separations are Cu2···O2A 3.228, Ag1···O1A 2.910, Cu2···N4A 3.210 Å (longer than the Cu−Cu 2.986–2.993 Å), Ag4···O2 2.717, Ag6···O3 3.025 Å for **1**–**5**, respectively, comparable or longer than the nonbonding distances between corresponding atoms. Most of these contacts are not consistent with displacements of the metal centers (except **1** and **2**), while the shortest metal–metal contacts are (most displaced metals: Cu2, Ag1, Cu1, Ag1, Ag5 for **1**–**5**, respectively). Assignment of the decreasing trend for the short interdimer metal–metal contacts to intermolecular metal–ligand attractive interactions is thus unlikely. The electrostatic attraction should not predominate such a structural change trend either, since the charge distributions of these $[M_2L_2]$ molecules should be rather similar (electronegativity for copper and silver 1.90 and 1.93, respectively).[20] Actually, the rich (slipped or rotated) conformations of the dimers-of-dimers rather than ideally eclipsed ones should be assigned to the geometric requirement of face-to-face π–π interaction.

Are these metal–metal contacts supported by face-to-face π–π interactions? Intermolecular aurophilic and hydrogen-bonding interactions in the same supramolecular motif can be cooperative[7] or competitive.[8] Such examples of coexisting intermolecular aurophilicity and hydrogen bonding are consistent with their comparable stabilization energy. The face-to-face π–π interaction is another important noncovalent intermolecular force in supramolecular chemistry.[21–23] However, coexisting intermolecular metallophilic and face-to-face π–π interactions between d^{10} complexes are rare, which may be denoted as "π–π-stacking supported metallophilic interactions".[4,5,13] Although a precise understanding of the origins and strength of π–π interactions is not yet available, a simple charge distribution model is widely accepted to qualitatively explain their stabilization energy.[21] Both experimental and theoretical studies reveal that two arene moieties would adopt a parallel offset conformation with an interplanar distance about 3.4–3.6 Å (longer than commonly accepted close metallophilicity) to reach the energy minimum (2–3 $kcal\,mol^{-1}$ for a benzene dimer).[21,22] The energy curve can remain negative upon slight deviation from the most stable conformation (energy minimum or equilibrium distance). However, the system should have a trend to reach the most stable conformation without other interference. We call the system "repulsive" when the distance is shorter than the equilibrium one, and vice versa. In other words, individual fragments can simultaneously contribute energy to stabilize the system and behave as repulsive. Generally, aromatic ligands are polarized by heteroatoms and/or metal coordination, thus the parallel offset conformation can be further divided into two types, that is, head-to-tail and head-to-head alignments. The head-to-tail alignment is more energetically favorable than the head-to-head one; this preference can easily be explained by charge distribution theory and demonstrated by a large number of examples. The equilibrium distance for a head-to-head alignment should be significantly lengthened, with respect to a head-to-tail one. Few face-

Table 1. Selected geometric parameters [Å] for oligomers-of-dimers in **1**–**5**.

	1	**2**	**3**	**4**	**5**
intramolecular M−M distances	2.674(2) Cu1−Cu2	2.7903(4) Ag1−Ag2	2.5790(4) Cu1−Cu2	2.7886(5) Ag1−Ag2	2.7450(4) Ag1−Ag2
				2.7963(5) Ag3−Ag4	2.7459(4) Ag3−Ag4
					2.7487(4) Ag5−Ag6
intermolecular M−M distances	3.595(3) Cu1−Cu2A	3.1994(5) Ag1−Ag2A	2.9862(5) Cu1−Cu1A	3.0228(5) Ag1−Ag3	3.1727(4) Ag2−Ag4
	3.595(3) Cu2−Cu1A	3.1994(5) Ag2−Ag1A	2.9934(4) Cu1−Cu2A	3.0809(5) Ag1−Ag4	3.5538(4) Ag1−Ag3
	4.310(3) Cu1−Cu1A	4.2015(6) Ag2−Ag2A	2.9934(4) Cu2−Cu1A	3.0921(5) Ag2−Ag3	3.5549(4) Ag1−Ag4
	4.645(4) Cu2−Cu2A	4.2884(7) Ag1−Ag1A	4.7230(5) Cu2−Cu2A	3.9355(5) Ag2−Ag4	3.8233(4) Ag2−Ag3
					3.1713(4) Ag3−Ag5
					3.2739(4) Ag4−Ag5
					3.5347(4) Ag4−Ag6
					4.0441(5) Ag3−Ag6
average	4.036	3.722	3.424	3.283	3.526, 3.501
deviation ($[M_2L_2]$)	0.056	0.094	0.096	0.139, 0.144	0.090, 0.028, 0.132
deviation (metal)	0.069 Cu1	0.238 Ag1	0.326 Cu1	0.459 Ag1	0.244 Ag1
	0.133 Cu2	0.228 Ag2	0.261 Cu2	0.307 Ag2	0.286 Ag2
				0.360 Ag3	0.022 Ag3
				0.329 Ag4	−0.024 Ag4
					0.433 Ag5
					0.229 Ag6
average	0.101	0.233	0.293	0.364	0.199
shortest intermolecular M−L distances	3.228 Cu2···O2A	2.910 Ag1···O1A	3.210 Cu2···N2	2.717 Ag4···O2	3.064 Ag3···O6
	3.253 Cu1···N3A	3.048 Ag2···N1A	3.546 Cu1···O1	2.799 Ag2···O4	3.071 Ag2···O3

to-face π–π interactions featuring head-to-head alignments are found when the aromatic fragments are supported by other interactions such as covalent bonds, coordination bonds, or metal–metal interactions.[13,21b]

The ophen ligand should adopt more significant π–π interactions than obpy due to their difference in conjugation size and rigidity,[22] similar to phen versus bpy.[23] On the other hand, both the ophen and obpy ligands are less favorable towards π–π interactions than phen and bpy, respectively, since the anions are more electron rich (Figure S4 in the Supporting Information).[21b] However, as observed in the four $[M_2L_2]$ dimers in **1**–**4**, intermolecular M−M separations decrease as the ligand changes from ophen to obpy when keeping the metal ions unchanged (3.595 to 2.986 Å for $[Cu_2L_2]$, 3.199 to 3.037 Å for $[Ag_2L_2]$). Therefore the short intermolecular M−M separations observed in **2**–**5** cannot be supported by attractive π–π interactions. The two dominant intermolecular interactions in these very closely packed oligomers-of-dimers are actually competitive: attractive metallophilicity and repulsive π–π interactions. It is worth noting that the number of overlapped six-membered aromatic rings are about six in **1** and **2**, four in **3**, and three in **4**, and such numbers follow the same trend as interdimer M−M distances (average interdimer M−M distances: 4.036, 3.722, 3.424 and 3.283 for **1**–**4**, respectively) in the corresponding complexes. All ophen and obpy fragments possess head-to-head alignments in **1**–**5**, whereas head-to-tail ones were found in the free ligands and other metal complexes reported by us previously.[18c] This observation indicates that the more significant interdimer π–π interactions disfavor stronger interdimer metallophilic interactions, and that these oligomers-of-dimers are equilibrium structures upon competition of the interdimer metallophilic and π–π interactions. Therefore, similar to the competitive phenomena found to exist between aurophilic and hydrogen-bonding interactions in the same motifs,[8] it may be concluded that the strengths of metallophilic and π–π interactions in these structures are also comparable. Based on our observation, the argentophilicity can also be qualitatively estimated to be stronger than the cuprophilicity. Although this idea has already been predicted by theoretical calculations,[16] it has not yet been verified by experiment and is under question.[17b] In complex **5**, the coexistence of a highly planar $[Ag_2(obpy)_2]$ molecule (middle) and two distorted ones (outer) with their Ag^I atoms displaced toward the middle molecule further indicates the distortion of the outer $[Ag_2(obpy)_2]$ molecule to be attributed to the intermolecular argentophilicity, and therefore supports our suggestion that the aggregation of the dimeric $[M_2L_2]$ molecules favored by of relatively stronger metallophilic and weaker π–π interactions.

It is easy to understand that face-to-face π–π interactions would usually hinder instead of support a close metallophilic interaction (typically less than 3.2 Å) to aromatic-containing planar molecules for several reasons. As shown in Figure 7, a decrease of the plane-to-plane distance from the equilibrium distance for the face-to-face π–π interactions (3.4–3.6 Å) is unfavorable in energy.[21] The conformation needed for a close metal–metal contact also disfavors attractive π–π interactions, since the head-to-head alignment of the polar aromatic moieties induces repulsive π–π interactions.[21a,b] These two kinds of distinct supramolecular interactions would be

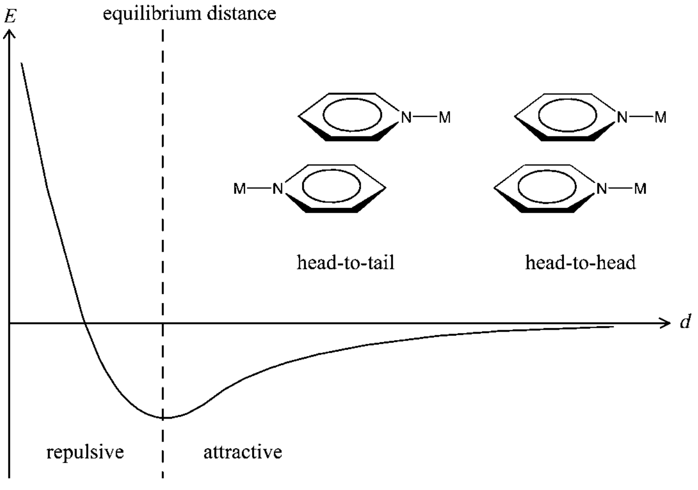

Figure 7. Schematic diagram of the energy versus distance for face-to-face π–π interaction (inset: two possible orientations for face-to-face π–π interactions of polarized aromatics).

combined in the same motif if the attractive metallophilic interaction is strong enough to compete against the repulsive interaction arising from the face-to-face π–π stacking, as exemplified in the extended structures of triangle-like planar trinuclear d^{10} metal complexes bridged by π-containing ligands. These triangles are usually associated through only two of the three metal centers, adopting staggered conformations to avoid significant π–π overlap.[4] In addition to the usual metal–metal interaction types of the triangles, a short Au−Au interaction (3.146(3) Å) accompanied with some extent of π–π overlaps extend $[Au_3(NC_5H_4)_3]$ molecules into a chain.[4e] When the conjugation size of the bridging ligands decreases, that is, six- to five-membered rings, the expected eclipsed conformations of these triangles has appeared in the literature. However, the shortest intermolecular Au−Au separation in these conformations is 3.318 Å.[4c] Shorter intermolecular Au−Au separations were found in almost eclipsed structures of $[Au_3(MeN{=}COEt)_3]$ (3.220 to 3.233 Å), in which the π system of the bridging ligand has only a single C=N double bond.[4d] In the infinite stacking structure of $[Au_3(MeN{=}COMe)_3]$, intermolecular Au−Au contacts are identical (3.346 Å) and longer than those of the dimers.[4f] It is evident that the trend implied by the aggregation of these gold(I) triangles and $[M_2L_2]$ molecules in this work is in good agreement. Other d^{10} metal complexes featuring both ligand-unsupported metallophilic and π–π interactions in which the metal–metal separations are relatively long are rare.[13] Instead, linear two-coordinate mononuclear complexes tend to aggregate perpendicularly to each other in order to reduce repulsion between the ligands.

It has been noted that not only the ligands, but also the molecular topologies affect the capability of metallophilic interactions.[16,17] Three- or four-coordinate d^{10} metal complexes rarely feature ligand-unsupported metallophilic interactions; this fact may be ascribed partly to their stereorepulsions compared with the two-coordinate complexes. The molecular topology of $[M_2L_2]$ complexes is entirely different to other molecular building blocks featuring ligand-unsupported metal–metal interactions, such as the well-known linear two-coordinate mononuclear and triangle-like trinuclear ones. The metal centers in $[Ag_3\{2\text{-}[3(5)\text{-pz}]py\}_3]_2$ and $[Cu_3\{2\text{-}[3(5)\text{-pz}]py\}_3]_2$ have T-shaped coordination environments, but their trinuclear configurations are different to that of $[M_2L_2]$.

Theoretical studies: To further verify our arguments, geometry optimizations and binding-energy calculations for the four dimers-of-dimers were performed at the Perdew–Burke–Ernzerhof (PBE) density functional theory[24] level by use of the double-ζ Salter-type (STO) basis set plus polarization functions (DZP), which has been proved successful in studying weak interactions.[25,26] The calculation of the binding energies for benzene, naphthalene dimers, and a naphthalene–anthracene complex were further tested at the PBE/DZP level of theory. The binding energies obtained from the PBE/DZP level without correction for basis set superposition error (BSSE) agreed with those reported in the literature.[25] These results suggest that traditional BSSE corrections with the counterpoise method may not be applicable when using the PBE functional.

The calculated M−M distances and molecular geometries (see Supporting Information) are in accord with our X-ray experimental values (calculated intermolecular M−M distances, d, and binding energies, ΔE, for the four dimers-of-dimers are shown in Table 2). Although the optimized interdimer Cu−Cu distances (3.321 Å) for $[Cu_2(ophen)_2]_2$ are significantly shorter than the observed ones (3.595 Å), the numbers are still the longest in the four optimized structures. The lengthened intermolecular Cu−Cu separations in the crystal structure may indicate that other intermolecular interactions or crystal packing effects play a more important role in **1**, which is in accord with our deductions.

Table 2. Optimized intermolecular M−M distances [d, Å] and calculated binding energies [ΔE, kcal mol^{-1}] for four dimers-of-dimers in **1**–**4** at the density functional theory PBE/DZP and MP2/DZVP levels.

	$[Ag_2(obpy)_2]_2$		$[Ag_2(ophen)_2]_2$		$[Cu_2(obpy)_2]_2$		$[Cu_2(ophen)_2]_2$	
	d	ΔE	d	ΔE	d	ΔE	d	ΔE
PBE/DZP	3.078	−25.73	3.276	−24.62	2.870 3.019	−26.72	3.321	−24.35
MP2/DZVP		−25.88[a]						
exptl values	3.023		3.199		2.986 2.994		3.595	

[a] The geometry of $[Ag_2(obpy)_2]_2$ is from PBE/DZP optimization.

The large binding energies (−24.35 to −26.72 kcal mol^{-1}) for the four dimers-of-dimers indicate that the oligomerizations of these $[M_2L_2]$ molecules in such conformations are inherently energy favorable. Therefore, crystal packing effects are only partly responsible for our observations. The binding energies for $[M_2(ophen)_2]_2$ are also less than $[M_2(obpy)_2]_2$, which is consistent with the fact that the short intermolecular metal–metal contacts are not supported by face-to-face π–π interactions.

Our benchmark calculations for the binding energy of $[Ag_2(obpy)_2]_2$ also suggest that the PBE/DZP level without the BSSE correction gives results comparable with the MP2 BSSE correlation calculations; the value found at the PBE/DZP (without BSSE correction) is $-25.73\,kcal\,mol^{-1}$, very close to the MP2 with DZVP basis set[27] value (BSSE correction) of $-25.88\,kcal\,mol^{-1}$.

Conclusion

There are several important structural features found in complexes **1**–**5**: 1) similar $[M_2L_2]$ structures and extended packing patterns, 2) relatively short interdimer metal–metal separations, 3) distorted $[M_2L_2]$ molecules and head-to-head alignments of the aromatic ligands, and 4) shorter intermolecular M−M separations and more distortions when M changes from Cu to Ag and/or L changes from ophen to obpy.

Although crystal packing effects, metal–ligand, metal–metal, and ligand–ligand interactions may have effects in the formation of the above unusual features, the common crystal packing effects have been initially ruled out as dominant forces for our structural comparison strategy. Metal–ligand interactions may be comparatively important in some of these structures. However, such metal–ligand interaction can hardly account for the structural change from **1** to **2**, as well as the difference between **3** and the others. Hence the remaining metal–metal and π–π interactions should be responsible for the aggregation of these $[M_2L_2]$ molecules, since all of the above features can be rationalized by the competition between the metallophilic and π–π interactions.

Our structural investigation demonstrates that argentophilic and cuprophilic attractive interactions do play an essential role in the formation of $[M_2L_2]$ oligomers, as evident by the fact that both the short interdimer M−M distances, and the bent distortion of the originally planar dimers can be tuned by the variation of the ligand structures and/or metal ions. Such observations suggest a competition between the metallophilic and the π–π interactions, which is further supported by our DFT calculations. The strengths of intermolecular argentophilic/cuprophilic interactions presented in these $[M_2L_2]_n$ oligomers should be comparable to that of face-to-face π–π interaction.

Experimental Section

Materials and physical measurements: Commercially available reagents are used as received without further purification. Hophen was prepared by our previously reported method.[18d] Infrared spectra were obtained from KBr pellets on a Bruker EQUINOX 55 Fourier transform infrared spectrometer in the 400–4000 cm^{-1} region. Elemental analyses (C, H, N) were performed on a Perkin–Elmer 240 elemental analyzer. ESI-MS spectra were performed on a Thermo Finigan LCQ DECA XP ion-trap mass spectrometer.

$[Ag_2(ophen)_2]_2\cdot 6H_2O$ (2): A solution of Ag_2O (0.116 g, 0.5 mmol) in aqueous ammonia (25 %, 5 mL) or a solution of $AgNO_3$ (0.170 g, 1.0 mmol) in MeCN (5 mL) was added to a solution of Hophen (0.197 g, 1.0 mmol) in MeCN (5 mL). The resulting clear solution was left in the dark for several days to give pale-yellow needles (yield ca. 40–70 %). Elemental analysis calcd (%) for $C_{48}H_{40}Ag_4N_8O_{10}$: C 43.66, H 3.05, N 8.49; found: C 43.72, H 2.98, N 8.53; IR (KBr): $\tilde{\nu}=3355$ (m), 3031 (m), 1616 (s), 1588 (s), 1513 (s), 1480 (s), 1455 (s), 1420 (s), 1383 (s), 1300 (m), 1138 (m), 935 (m), 838 (s), 728 (s), 703 (m), 661 (m), 638 (m), 480 cm^{-1} (m).

$[Cu_2(obpy)_2]_2$ (3): Reaction of a mixture of $Cu(OAc)_2\cdot H_2O$ (0.200 g, 1.0 mmol), bpy (0.156 g, 1 mmol), NaOH (0.040 g, 1 mmol) and H_2O (10 mL) in a 23 mL Teflon-lined bomb at 160 °C for 80 h afforded black platelike crystals (yield ca. 30 %).[18a,b] Elemental analysis calcd (%) for $C_{40}H_{28}Cu_4N_8O_4$: C 51.17, H 3.01, N 11.93; found: C 51.14, H 3.05, N 11.89; IR (KBr): $\tilde{\nu}=3056$ (m), 3015 (m), 1608 (s), 1539 (s), 1486 (s), 1458 (s), 1376 (s), 1284 (m), 1151 (m), 998 (m), 775 (s), 741 (m), 652 (m), 576 cm^{-1} (m).

Hobpy·1/6 benzene: Pale-yellow powder Hobpy was prepared similarly to Hophen by demetallation of **3** according to reported procedures[18d] (yield >95 %); M.p. 115–116 °C, ESI-MS: m/z: 173 $[M+H]^+$; crystals of Hobpy·1/6 benzene suitable for X-ray analysis were grown from a hot solution of Hobpy in benzene. Elemental analysis calcd (%) for $C_{11}H_9N_2O$: C 71.34, H 4.90, N 15.13; found: C 71.30, H 4.94, N 15.19; IR (KBr): $\tilde{\nu}=$ 3060 (m), 2950 (m), 2799 (w), 1651 (vs), 1607 (s), 1576 (s), 1484 (s), 1435 (m), 1303 (w), 1250 (w), 1149 (w), 1092 (w), 989 (m), 885 (m), 781 (s), 560 cm^{-1} (m).

$[Ag_2(obpy)_2]_2\cdot 4.5H_2O\cdot 0.5DMF$ (4): A solution of Ag_2O (0.116 g, 0.5 mmol) in aqueous ammonia (25 %, 5 mL) or a solution of $AgNO_3$ (0.170 g, 1.0 mmol) in MeCN (5 mL) was added to a solution of Hobpy (0.177 g, 1.0 mmol) in DMF (5 mL). Diffusion of diethyl ether into the resulting clear solution gave colorless crystals (yield ca. 10–20 %). Elemental analysis calcd (%) for $C_{41.5}H_{40.5}Ag_4N_{8.5}O_9$: C 40.40, H 3.31, N 9.65; found: C 40.28, H 3.40, N 9.54; IR (KBr): $\tilde{\nu}=3387$ (m), 3056 (m), 3017 (m), 1656 (w), 1591 (s), 1481 (m), 1447 (s), 1367 (s), 1271 (m), 1156 (m), 991 (m), 771 (s), 738 (m), 651 (w), 593 cm^{-1} (w).

$[Ag_2(obpy)_2]_3\cdot 18H_2O$ (5): A solution of Ag_2O (0.116 g, 0.5 mmol) in aqueous ammonia (25 %, 5 mL) or a solution of $AgNO_3$ (0.170 g, 1.0 mmol) in MeCN (5 mL) was added to a solution of Hobpy (0.177 g, 1.0 mmol) in DMF (5 mL). The resulting clear solution was left standing in the dark for several days to give colorless platelike crystals (yield ca. 20–30 %). Elemental analysis calcd (%) for $C_{60}H_{78}Ag_6N_{12}O_{24}$: C 36.06, H 3.93, N 8.41; found: C 36.15, H 3.82, N 8.50; IR (KBr): $\tilde{\nu}=3294$ (m), 3061 (m), 3017 (m), 1591 (vs), 1540 (m), 1482 (vs), 1457 (vs), 1367 (s), 1273 (m), 1156 (m), 992 (m), 919 (w), 772 (s), 738 (m), 652 (m), 593 cm^{-1} (m).

X-ray crystallography: Diffraction intensities were collected at 123 K on a Bruker Smart APEX CCD area-detector diffractometer ($Mo_{K\alpha}$, λ 0.71073 Å). Absorption corrections were applied by using the multiscan program SADABS.[28] The structures were solved with direct methods and refined with a full-matrix least-squares technique with the SHELXTL program package.[29] Anisotropic thermal parameters were applied to all non-hydrogen atoms. The organic hydrogen atoms were generated geometrically (CH 0.96 Å); the aqua hydrogen atoms were located from difference maps and refined with isotropic temperature factors. Crystal data as well as details of data collection and refinements for the complexes are summarized in Table 3. The drawings were produced with SHELXTL.

CCDC 245547 to CCDC 245551 contain the supplementary crystallographic data for this paper. These data can be obtained free of charge from The Cambridge Crystallographic Data Centre via www.ccdc.cam.ac.uk/data_request/cif.

Computational details: The geometry optimizations and binding energy calculations were performed at the Perdew–Burke–Ernzerhof (PBE) density functional theory[24] level by use of the double-ζ Salter-type (STO) basis set plus polarization functions (DZP).

Table 3. Crystallographic data and structure refinements for Hobpy·1/6 benzene and **2**–**5**.

Compound	Hobpy·1/6benzene	**2**	**3**	**4**	**5**
formula	$C_{11}H_9N_2O$	$C_{48}H_{40}Ag_4N_8O_{10}$	$C_{40}H_{28}Cu_4N_8O_4$	$C_{41.5}H_{40.5}Ag_4N_{8.5}O_9$	$C_{60}H_{78}Ag_6N_{12}O_{24}$
a [Å]	30.206(1)	20.9511(8)	11.0706(6)	11.2102(5)	13.7559(7)
b [Å]	30.206(1)	26.181(1)	11.7020(6)	16.1189(7)	19.283(1)
c [Å]	5.1177(4)	8.2369(4)	13.5602(8)	23.078(1)	26.239(1)
β [°]	90	100.282(2)	106.768(3)	91.178(2)	95.405(1)
V [Å^3]	4044.0(4)	4445.6(4)	1682.0(2)	4169.2(6)	6928.9(6)
Z	18	4	2	4	4
M_r	185.21	1320.36	938.86	1233.80	1998.56
space group	$R-3$ (No. 148)	$C2/c$ (No. 15)	$P2_1/n$ (No. 14)	$P2_1/n$ (No. 14)	$P2_1/c$ (No. 14)
ρ_{calcd} [g cm^{-13}]	1.369	1.973	1.854	1.966	1.916
μ (Mo$_{K\alpha}$) [mm^1]	0.9	1.808	2.555	1.919	1.750
$R1$ (all data)[a]	0.0622	0.0433	0.0354	0.0493	0.0499
wR_2 (all data)[b]	0.1337	0.0942	0.0791	0.0812	0.1069

[a] $R_1 = \Sigma||F_o - F_c||/\Sigma|F_o|$. [b] $wR_2 = [\Sigma w(F_o^2 - F_c^2)^2/\Sigma(F_o^2)^2]^{1/2}$.

The DFT calculations were performed with the PVM-parallelism ADF 2002.2 software package[30a] and the MP2 binding energy benchmark calculations with the Linda-parallelism Gaussian 98 program[30b] on a 16-nodes Beowulf Linux cluster computer system.

Acknowledgments

This work was supported by the National Natural Science Foundation of China (Grant No. 20131020), Ministry of Education of China (Grant No. 01134 and Grant No. 20020558024) and Guangdong Provincial Science and Technology Bureau.

---

[1] a) M. Jansen, *Angew. Chem.* **1987**, *99*, 1136; *Angew. Chem. Int. Ed. Engl.* **1987**, *26*, 1098; b) P. Pyykkö, *Chem. Rev.* **1997**, *97*, 597; c) C. Janiak, *Coord. Chem. Rev.* **1997**, *163*, 107 and refs cited therein.

[2] a) P. Pyykkö, *Angew. Chem.* **2002**, *114*, 3723; *Angew. Chem. Int. Ed.* **2002**, *41*, 3573; b) H. Schmidbaur, *Nature* **2001**, *413*, 31 and references therein.

[3] a) A. Hamel, N. W. Mitzel, H. Schmidbaur, *J. Am. Chem. Soc.* **2001**, *123*, 5106; b) A. A. Mohamed, J.-H. Chen, A. E. Bruce, M. R. M. Bruce, *Inorg. Chem.* **2003**, *42*, 2203.

[4] a) A. Burini, J. P. Fackler, Jr., R. Galassi, T. A. Grant, M. A. Omary, M. A. Rawashdeh-Omary, B. R. Pietroni, R. J. Staples, *J. Am. Chem. Soc.* **2000**, *122*, 11264; b) M. A. Rawashdeh-Omary, M. A. Omary, J. P. Fackler, Jr., *J. Am. Chem. Soc.* **2001**, *123*, 9689; c) G. Yang, R. G. Raptis, *Inorg. Chem.* **2003**, *42*, 261; d) M. M. Olmstead, F.-L. Jiang, S. Attar, A. L. Balch, *J. Am. Chem. Soc.* **2001**, *123*, 3260; e) A. Hayashi, M. M. Olmstead, S. Attar, A. L. Balch, *J. Am. Chem. Soc.* **2002**, *124*, 5791.

[5] a) R. J. Puddephatt, *Chem. Commun.* **1998**, 1055; b) L.-J. Hao, R. J. Lachicotte, H. J. Gysling, R. Eisenberg, *Inorg. Chem.* **1999**, *38*, 4616.

[6] a) D. E. Harwell, M. D. Mortimer, C. B. Knobler, F. A. L. Anet, M. F. Hawthorne, *J. Am. Chem. Soc.* **1996**, *118*, 2679; b) J. Zank, A. Schier, H. Schmidbaur, *J. Chem. Soc. Dalton Trans.* **1998**, 323.

[7] a) C. Hollatz, E. J. Schier, H. Schmidbaur, *J. Am. Chem. Soc.* **1997**, *119*, 8115; b) C. Hollatz, E. J. Schier, J. Riede, H. Schmidbaur, *J. Chem. Soc. Dalton Trans.* **1999**, 111; c) W. J. Hunks, M. C. Jennings, R. J. Puddephatt, *Inorg. Chem.* **2000**, *39*, 2699; d) F. Mendizabal, P. Pyykkö, N. Runeberg, *Chem. Phys. Lett.* **2003**, *370*, 733.

[8] a) A. Codina, E. J. Fernández, P. G. Jones, A. Laguna, J. M. López-de-Luzuriaga, M. Monge, M. E. Olmos, J. Pérez, M. A. Rodríguez, *J. Am. Chem. Soc.* **2002**, *124*, 6781; b) D. R. Smyth, J. Hester, V. G. Young, Jr., E. R. T. Tiekink, *CrystEngComm* **2002**, *4*, 517.

[9] a) F. A. Cotton, X. Feng, M. Matusz, R. Poli, *J. Am. Chem. Soc.* **1988**, *110*, 7077; b) E. J. Fernández, J. M. López-de-Luzuriaga, M. Monge, M. A. Rodriguez, O. Crespo, M. C. Gimeno, A. Laguna, P. G. Jones, *Inorg. Chem.* **1998**, *37*, 6002; c) J. El-Bahraoudi, J. M. Molina, D. P. Olea, *J. Phys. Chem. A* **1998**, *102*, 2443.

[10] a) M.- L. Tong, X.-M. Chen, B.-H. Ye, L.-N. Ji, *Angew. Chem.* **1999**, *111*, 2376; *Angew. Chem. Int. Ed.* **1999**, *38*, 2237; b) A. Galet, V. Niel, M. C. Munoz, J. A. Real, *J. Am. Chem. Soc.* **2003**, *125*, 14227.

[11] a) U. Siemeling, U. Vorfeld, B. Neumann, H.-G. Stammler, *Chem. Commun.* **1997**, 1723; b) J.-M. Poblet, M. Bénard, *Chem. Commun.* **1998**, 1179.

[12] a) X.- M. Chen, T. C. W. Mak, *J. Chem. Soc. Dalton Trans.* **1991**, 3253; b) N. Masciocchi, M. Moret, P. Cairati, A. Sironi, G. A. Ardizzoia, G. L. Monica, *J. Am. Chem. Soc.* **1994**, *116*, 7668; c) O. M. Yaghi, H. Li, *J. Am. Chem. Soc.* **1996**, *118*, 295; d) K. Singh, J. R. Long, P. Stavropoulos, *J. Am. Chem. Soc.* **1997**, *119*, 2942; e) L. Pan, E. B. Woodlock, X.-T. Wang, K.-C. Lam, A. L. Rheingold, *Chem. Commun.* **2001**, 1762; f) C. J. Shorrock, B.-Y. Xue, P. B. Kim, R. J. Batchelor, B. O. Patrick, D. B. Leznoff, *Inorg. Chem.* **2002**, *41*, 6743; g) S.-L. Zheng, M.-L. Tong, X.-M. Chen, S. W. Ng, *J. Chem. Soc. Dalton Trans.* **2002**, 360; h) O.-S. Jung, Y.-A. Lee, Y. J. Kim, J. Hong, *Cryst. Growth Des.* **2002**, *2*, 497.

[13] A. N. Khlobystov, A. J. Blake, N. R. Champness, D. A. Lemenovskii, A. G. Majouga, N. V. Zyk, M. Schröder, *Coord. Chem. Rev.* **2001**, *222*, 155 and refs cited therein.

[14] a) G. Margraf, J. W. Bats, M. Bolte, H.-W. Lerner, M. Wagner, *Chem. Commun.* **2003**, 956; b) R. D. Köhn, G. Seifert, Z. Pan, M. F. Mahon, G. Kociok-Köhn, *Angew. Chem.* **2003**, *115*, 818; *Angew. Chem. Int. Ed.* **2003**, *42*, 793; c) G. Boche, F. Bosold, M. Marsch, K. Harms, *Angew. Chem.* **1998**, *110*, 1779; *Angew. Chem. Int. Ed.* **1998**, *37*, 1684; d) K. Singh, J. R. Long, P. Stavropoulos, *J. Am. Chem. Soc.* **1997**, *119*, 2942.

[15] a) C.-M. Che, M.-C. Tse, M. C. W. Chan, K.-K. Cheung, D. L. Phillips, K.-H. Leung, *J. Am. Chem. Soc.* **2000**, *122*, 2464; b) C.-M. Che, Z. Mao, V. M. Miskowski, M.-C. Tse, C.-K. Chan, K.-K. Cheung, D. L. Phillips, K.-H. Leung, *Angew. Chem.* **2000**, *112*, 4250; *Angew. Chem. Int. Ed.* **2000**, *39*, 4084.

[16] a) H. L. Hermann, G. Boche, P. Schwerdtfeger, *Chem. Eur. J.* **2001**, *7*, 5333; b) L. Magnko, M. Schweizer, G. Rauhut, M. Schütz, H. Stoll, H.-J. Werner, *Phys. Chem. Chem. Phys.* **2002**, *4*, 1006.

[17] a) X.-Y. Liu, F. Mota, P. Alemany, J. J. Novoa, S. Alvarez, *Chem. Commun.* **1998**, 1149; b) E. O'Grady, N. Kaltsoyannis, *Phys. Chem. Chem. Phys.* **2004**, *6*, 680.

[18] a) X.-M. Zhang, M.-L. Tong, X.-M. Chen, *Angew. Chem.* **2002**, *114*, 1071; *Angew. Chem. Int. Ed.* **2002**, *41*, 1029; b) X.-M. Zhang, M.-L. Tong, M.-L. Gong, H.-K. Lee, L. Luo, K.-F. Li, Y.-X. Tong, X.-M. Chen, *Chem. Eur. J.* **2002**, *8*, 3187; c) S.-L. Zheng, J.-P. Zhang, W.-T. Wong, X.-M. Chen, *J. Am. Chem. Soc.* **2003**, *125*, 6882; d) S.-L. Zheng, J.-P. Zhang, X.-M. Chen, Z.-L. Huang, Z.-Y. Lin, W.-T. Wong, *Chem. Eur. J.* **2003**, *9*, 3888.

[19] A. Bondi, *J. Phys. Chem.* **1964**, *68*, 441.

[20] J. A. D. Dean, *Lange's Handbook of Chemistry*, 15th ed., McGraw-Hill, Beijing, **1999**.

[21] a) C. A. Hunter, J. K. M. Sanders, *J. Am. Chem. Soc.* **1990**, *112*, 5525; b) C. Janiak, *J. Chem. Soc. Dalton Trans.* **2000**, 3885; c) M. O. Sinnokrot, E. F. Valeev, C. D. Sherrill, *J. Am. Chem. Soc.* **2002**, *124*, 10887 and refs cited therein.

[22] J. W. Steed, J. L. Atwood, *Supramolecular Chemistry*, Wiley, Chichester, **2000**.

[23] V. Russell, M. Scudder, I. Dance, *J. Chem. Soc. Dalton Trans.* **2001**, 789 and references therein.

[24] a) J. P. Perdew, K. Burke, M. Ernzerhof, *Phys. Rev. Lett.* **1996**, *77*, 3865; b) J. P. Perdew, K. Burke, M. Ernzerhof, *Phys. Rev. Lett.* **1997**, *78*, 1396.

[25] Y.-B. Wang, Z.-Y. Lin, *J. Am. Chem. Soc.* **2003**, *125*, 6072.

[26] a) C. Adamo, M. Cossi, N. Rega, V. Barone, *Theoretical and Computational Chemistry, Vol. 9* (Ed.: L. A. Eriksson), Elsevier, Amsterdam, **2001**, p. 467; b) R. Improta, V. Barone, K. N. Kudin, G. E. Scuseria, *J. Am. Chem. Soc.* **2001**, *123*, 3311.

[27] N. Godbout, D. R. Salahub, J. Andzelm, E. Wimmer, *Can. J. Chem.* **1992**, *70*, 560.

[28] R. Blessing, *Acta Crystallogr. Sect. A* **1995**, *51*, 33.

[29] G. M. Sheldrick, SHELXTL, Version 6.10, Siemens Industrial Automation, Madison, Wisconsin (USA), **2000**.

[30] a) G. T. Velde, F. M. Bickelhaupt, S. J. A. van Gisbergen, C. F. Guerra, E. J. Baerends, J. G. Snijders, T. Ziegler, *J. Comput. Chem.* **2001**, *22*, 931; b) Gaussian98 (Revision A11.3), M. J. Frisch, G. W. Trucks, H. B. Schlegel, G. E. Scuseria, M. A. Robb, J. R. Cheeseman, V. G. Zakrzewski, J. A. Montgomery, R. E. Stratmann, J. C. Burant, S. Dapprich, J. M. Millam, A. D. Daniels, K. N. Kudin, M. C. Strain, O. Farkas, J. Tomasi, V. Barone, M. Cossi, R. Cammi, B. Mennucci, C. Pomelli, C. Adamo, S. Clifford, J. Ochterski, G. A. Petersson, P. Y. Ayala, Q. Cui, K. Morokuma, D. K. Malick, A. D. Rabuck, K. Raghavachari, J. B. Foresman, J. Cioslowski, J. V. Ortiz, B. B. Stefanov, G. Liu, A. Liashenko, P. Piskorz, I. Komaromi, R. Gomperts, R. L. Martin, D. J. Fox, T. Keith, M. A. Al-Laham, C. Y. Peng, A. Nanayakkara, C. Gonzalez, M. Challacombe, P. M. W. Gill, B. G. Johnson, W. Chen, M. W. Wong, J. L. Andres, M. Head-Gordon, E. S. Replogle, J. A. Pople, Gaussian,, Pittsburgh, PA, **1998**.

Received: July 22, 2004